

Dynamic Correction of Higher-Order Deflection Aberrations in the Environmental SEM

Martin Oral¹, Vilém Neděla¹ and Gerasimos D. Danilatos²

¹ Institute of Scientific Instruments, AS CR, Královopolská 147, 612 64 Brno, Czech Republic

² ESEM Research Laboratory, 28 Wallis Parade, North Bondi, NSW 2026, Australia

Introduction

The two-stage deflection system is standard in the scanning electron microscope. It utilizes two deflectors located in front of the final lens. The excitation of the deflection stages are in such a proportion that the beam enters the final lens so that the asymptote of the central ray crosses the optical axis at (or close to) the object nodal point of the lens [Vol. 2 of 1]. The precise position may be subject to an optimization [2,3]. The deflected axial ray behind the lens then appears to originate from an axial point, known as the (virtual) pivot or rocking point.

An important parameter in environmental scanning electron microscopy (ESEM) is the environmental distance between the sample and the pressure limiting aperture (PLA). To minimize interaction of the primary electron beam with the gaseous environment, the PLA should be as close as possible to the sample. Additionally, its pressure limiting effect is better for smaller diameters. To minimize vignetting caused by striking the edge of the aperture by the deflected beam at high deflection angles (Figure 1) the PLA should be close to the real pivot point (where the central trajectory physically crosses the axis). However, that position usually increases the environmental distance unfavourably. Up to date, the obvious solution practiced by manufacturers of ESEM is to significantly increase the diameter of PLA. However, this introduces severe disadvantages, such as electron beam loss, increased pumping, restricted pressure range, inaccessible low energy beam at high pressure and overall limited instrument performance [4,5].

A much better solution to the above problem has been proposed by Danilatos [4], which has motivated the present work. The key idea is to move the pivot point of the deflection close to or at the PLA. While this can be achieved simply by altering the ratio between the deflection stage excitations, it is detrimental to the deflection aberrations, with even the higher order aberrations becoming significant (see the column labelled “Before correction” in Table 1). The reasons for the increase are the increase of the off-axial distance at which the trajectories enter the final lens and the increase of the angle at which the beam needs to be deflected to achieve the same deflection distance.

Some deflection aberrations can be eliminated by dynamic corrections [6], namely the deflection distortion, field curvature and astigmatism. Incidentally, these aberrations are typically the most serious ones. As the distortion of any order depends just on the deflection, it is corrected using non-linear deflection signals. Field curvature and astigmatism of the third-order can be corrected using dynamic (deflection-dependent) focus lens and a dynamic stigmator. The dynamic stigmator is a quadrupole lens which must enable not only the change of its optical power but also the change of the azimuthal orientation of its field (electronic rotation about the optical axis). Fifth-order field curvature and astigmatism can then be corrected by another pair of a dynamic lens and a stigmator [7].

The methods of correction outlined in [6] and [7] aim at eliminating each order of field curvature and astigmatism successively by a separate pair of dynamic focus lens and a dynamic stigmator per aberration order.

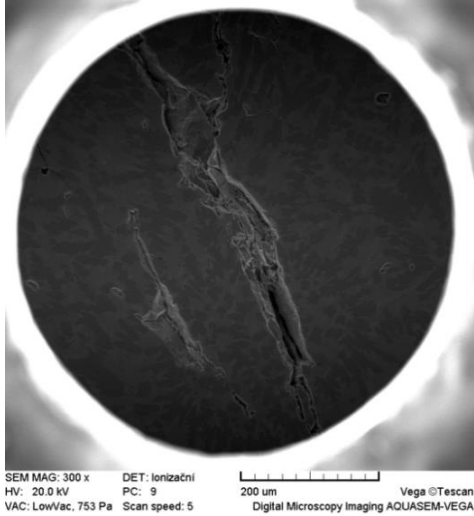


Figure 1: The field of view in the AquaSEM-Vega (ISI Brno) limited by the first pressure limiting aperture.

That complicates realization or adaptation of an instrument – the optical column and the electronics. In this paper we investigate the possibility of minimizing all orders of field curvature and astigmatism simultaneously using just a single dynamic focus lens and a single stigmator instead of eliminating each order separately.

The Method

We assume rotationally invariant magnetic deflectors [2] in front of the final magnetic lens (Figure 2). The deflectors are driven by deflection currents I_1 and I_2 , respectively. The quantities I are complex numbers, with their real and imaginary part denoting the current in a deflector creating the dipole field in the directions of the x and y axes, respectively. The final lens essentially images an intermediate crossover from the axial position z_o onto the sample.

The paraxial properties of the two deflection stages and the lens are:

$g(z), h(z)$: principal rays of the lens without the deflection fields ($g(z_o)=h'(z_o)=1, g'(z_o)=h(z_o)=0$),

$\theta(z)$: paraxial image rotation angle in the lens without the deflection fields,

$\gamma_1(z)$: deflected axial trajectory ($\gamma_1(z_o)=\gamma_1'(z_o)=0$) with $I_1=1$ and $I_2=0$ and the lens activated,

$\gamma_2(z)$: deflected axial trajectory ($\gamma_2(z_o)=\gamma_2'(z_o)=0$) with $I_2=1$ and $I_1=0$ and the lens activated,

where the prime denotes the derivative with respect to z . As the general deflected axial trajectory is $\gamma(z) = I_1\gamma_1(z) + I_2\gamma_2(z)$, the condition $\gamma(z_p) = 0$ for a pivot point at z_p sets the complex ratio between the currents:

$$I_2/I_1 = -\gamma_1(z_p)/\gamma_2(z_p) \tag{1}$$

The geometrical aberration polynomial of order N can be written as:

$$w(z) = e^{i\theta(z)} \sum_{a+b+c+d+k+l \leq N} C_{abcdkl}(z) \alpha^a \bar{\alpha}^b \beta^c \bar{\beta}^d \gamma^k(z) \bar{\gamma}^l(z) \tag{2}$$

where α and β are the complex slope $x' + iy'$ and the complex position $x + iy$ in the object plane $z = z_o$, respectively, $w(z)$ is the complex position in a plane $z = \text{const}$, and the bar denotes a complex conjugate. The coefficients C_{abcdkl} are defined by the optical system and can be calculated by various methods, including aberration integrals [2,3], the differential algebra method [9], or regression analysis [11], which is our method of choice.

The following consideration can be made about the symmetry of the system: if the object is rotated by an angle about the axis and the deflection fields are rotated about the same angle, then the system produces an image identical to that before the rotations, only rotated by the same angle. This leads to the condition:

$$a - b + c - d + k - l = 1 \tag{3}$$

This condition allows only certain terms to be present in the polynomial (2). Although it is similar to that found in Vol. 1 of [1] for the rotationally symmetric case, it has never been published for systems containing deflectors considering their arbitrary rotation as part of the symmetry relation.

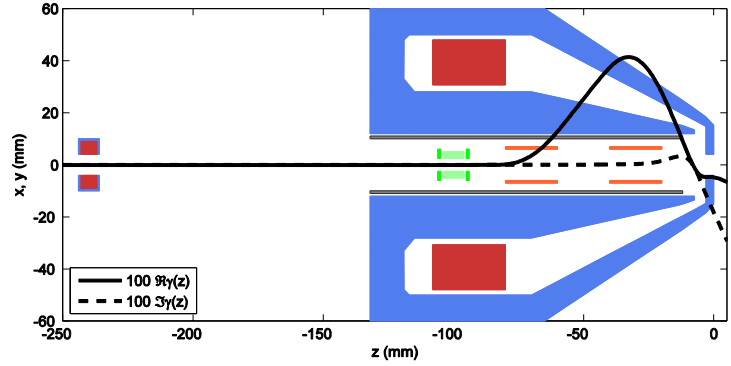


Figure 2: Optical system configuration: the bore in the inner pole piece contains a ferrite shielding inside which, from right to left, are two rotationally invariant pre-lens deflector stages and the dynamic stigmator. There is the dynamic focus lens on the far left. The curves are the components (the real and imaginary part) of the deflected axial trajectory plotted for the optimal pivot point position.

Let us assume that the correcting elements, the dynamic stigmator and the dynamic focus lens, are weak and their optics can be described just by paraxial terms. The combination of a stigmator with the azimuthal rotation ϵ and a lens modifies the position and the slope as follows:

$$\begin{aligned} \alpha &= (Q_{a1}\alpha_o + Q_{a2}\bar{\alpha}_o e^{2i\epsilon} + Q_{a3}\beta_o + Q_{a4}\bar{\beta}_o e^{2i\epsilon})e^{i\theta_l}, \\ \beta &= (Q_{b1}\alpha_o + Q_{b2}\bar{\alpha}_o e^{2i\epsilon} + Q_{b3}\beta_o + Q_{b4}\bar{\beta}_o e^{2i\epsilon})e^{i\theta_l} \end{aligned} \tag{4}$$

where θ_l is the image rotation of the dynamic focus lens, α_o is the slope and β_o is the position of the trajectory asymptotes in the object plane z_o and the resulting α and β refer to the trajectory asymptotes at z_o again of the trajectories behind the two correcting elements as they enter the deflectors and the final lens. As a quadrupole has two symmetry planes, the coefficients Q in eqs. (4) must be real and they can be determined from the cardinal elements of the dynamic quadrupole lens and the dynamic focus lens.

Substituting Eqs. (4) into the polynomial (2) will result in an expression of the entire sequence of the optical elements (the dynamic stigmator, the dynamic focus lens, the two deflectors and the final lens). As we are primarily interested in affecting field curvature and coma, we investigate just the terms in Eq. (2) that are linear in α , $\bar{\alpha}$, β and $\bar{\beta}$. We get an expression of the form:

$$\alpha F_a(\gamma, \bar{\gamma}) + \bar{\alpha} A_a(\gamma, \bar{\gamma}) + \beta F_b(\gamma, \bar{\gamma}) + \bar{\beta} A_b(\gamma, \bar{\gamma}), \tag{5}$$

where we have omitted the rotation factor $e^{i\theta(z)}$ which is further unimportant, and the coefficients are specifically:

$$\begin{aligned} F_a &= C_{100000} + C_{100011}\gamma\bar{\gamma} + C_{100022}\gamma^2\bar{\gamma}^2 + C_{100033}\gamma^3\bar{\gamma}^3 + \dots \\ A_a &= C_{010020}\gamma^2 + C_{010031}\gamma^3\bar{\gamma}^1 + C_{010042}\gamma^4\bar{\gamma}^2 + \dots \\ F_b &= C_{000100} + C_{000101}\gamma\bar{\gamma} + C_{000102}\gamma^2\bar{\gamma}^2 + C_{000103}\gamma^3\bar{\gamma}^3 + \dots \\ A_b &= C_{000120}\gamma^2 + C_{000131}\gamma^3\bar{\gamma}^1 + C_{000142}\gamma^4\bar{\gamma}^2 + \dots \end{aligned} \tag{6}$$

Keeping in mind that the coefficients $C(z)$ and the paraxial deflection γ is still a function of z , we retain the possibility of minimizing the two aberration types in any plane. However, note that in the Gaussian image plane $C_{100000} = 0$ and C_{000100} has the meaning of the direct magnification of the final lens. The coefficients C_{010000} and C_{000100} are not present in Eqs. (6), since they are zero as per condition (3). To find the effect of the correcting elements on overall field curvature and astigmatism, we substitute Eqs. (4)

into the expression (6). The aberration terms dependent on α_o and $\bar{\alpha}_o$ are of the form

$$\alpha_o U + \bar{\alpha}_o V, \quad (7)$$

where the complex factors U and V depend on the coefficients in Eq. (4) and those defined by Eq. (6). Now suppose that we send a cone of trajectories, $\alpha_o := a \cdot e^{it}$, with a being a real constant and t is a parameter running from 0 to 2π , from the object plane into the system. Eq. (7) becomes a parametric equation of a closed, ellipse-like curve. For known aberration coefficients in Eq. (4), U and V become functions of the dynamic focus current and the dynamic stigmator voltage. To minimize the effect of field curvature and astigmatism, the size of the closed curve needs to be minimized. While this can be done analytically, it leads to lengthy algebraic expressions for the excitation current of dynamic focus lens and the voltage of the dynamic stigmator and its rotation. Therefore, we have opted for a numerical solution using the simplex minimization search method.

Calculation Example

The configuration in Figure 2 was modelled using the EOD software [12]. The field of the lens was computed, taking the magnetic saturation into account, so that a virtual crossover at $z_o = -150$ mm is imaged to $z_i = 5$ mm. The optimal pivot point is located at $z = -7.5$ mm, but to investigate the effect of the deflection aberration and their reduction using the outlined method, it was moved to $z = 0$. For that position the magnitude of the current in the second deflector needs to be $1.7697 \times$ of that in the first one, and the dipole field in the second deflector needs to be rotated by 88.86 degrees relative to the first one (set via Eq. 1). The aberration coefficients of orders up to 7 were computed using the regression analysis [11] for 1600 trajectories computed in EOD (Figure 3). The dynamic focus lens and the dynamic stigmator (Figure 2) were placed to $z = -240$ mm and $z = -90$ mm, respectively. Their cardinal elements were obtained using the EOD. Their calculated excitation parameters are in Figure 4. The effect of the method on the testing optical system is documented in Table 1 and Figure 5. Apart from the field and trajectory calculations that were performed in the EOD, other calculations were programmed and carried out in Matlab.

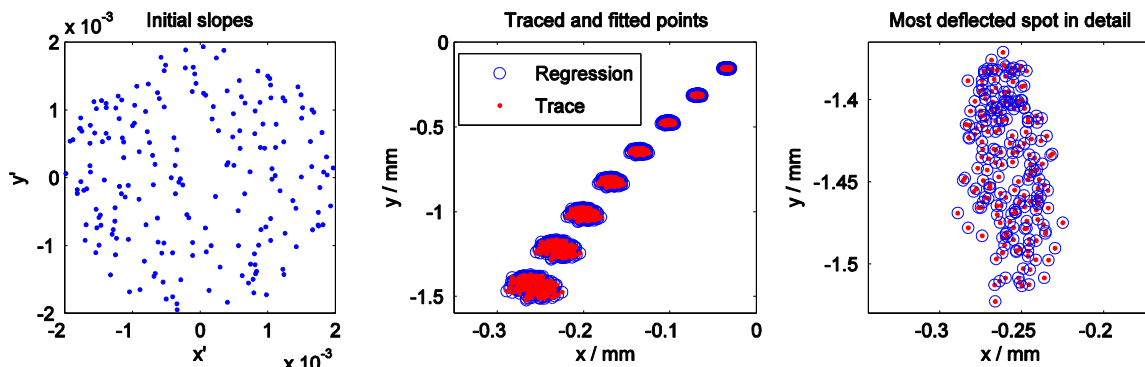


Figure 3. Initial conditions and results of ray tracing and regression analysis used to obtain the aberration coefficients of up to the 7th order. A set of 200 trajectories were traced for 8 different deflection currents from 1 At to 8 At in 1At steps. The complex slopes (left) and the initial positions (not plotted) were generated randomly with a uniform distribution over a circle in the complex plane with the maximal modulus of 0.002 and $0.05 \mu\text{m}$, respectively. The traced and the fitted positions in the Gaussian image plane are plotted in an overall view (centre) and a selected set in detail (right), showing a very good agreement between the traced data (dots) and the fit (circles).

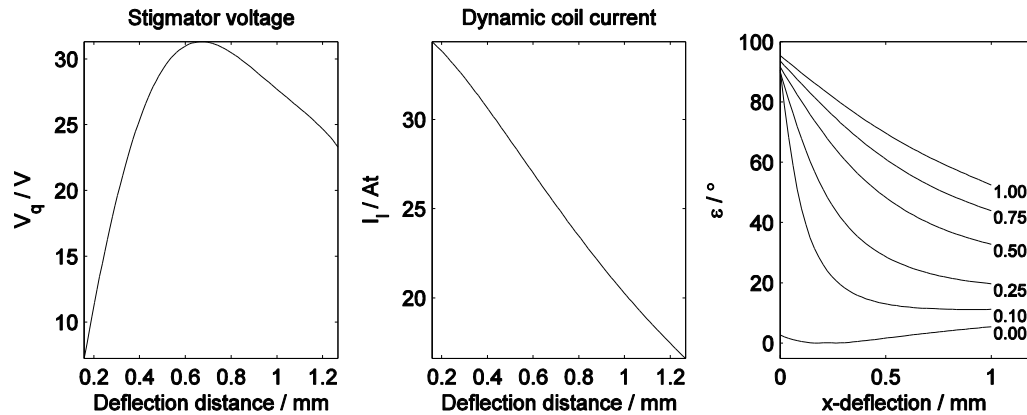


Figure 4. Calculated dependencies of the correcting element parameters on the paraxial deflection distance (stigmator voltage and dynamic coil current) and paraxial deflection position (stigmator rotation; the numbers next to the curves indicate the y coordinate in millimeters).

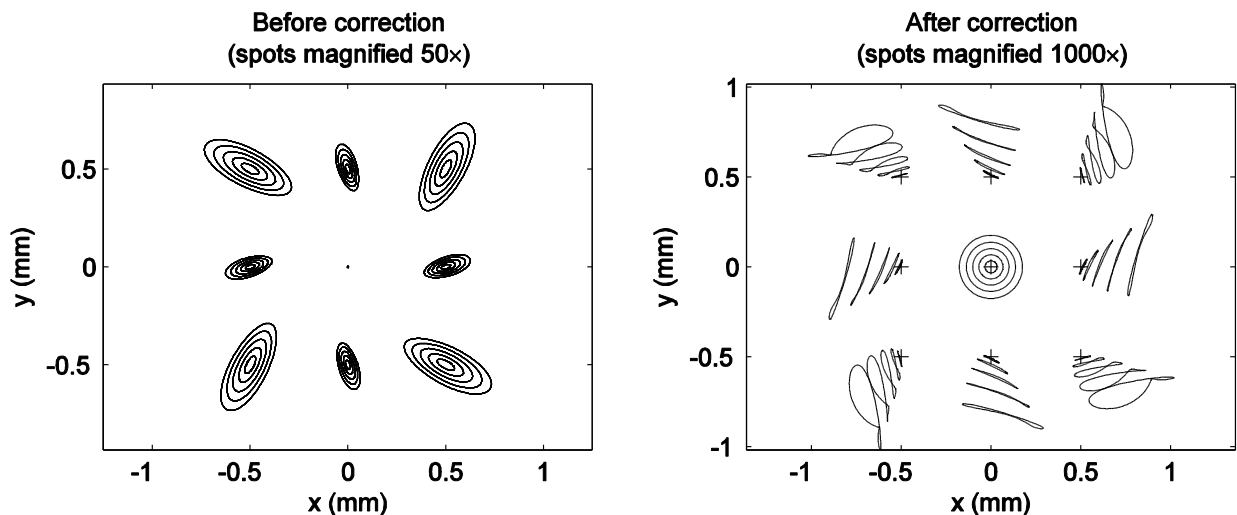


Figure 5. Aberration figures of all aberration minus the paraxial deflection and deflection distortion in a 3×3 raster of a 1mm field of view. The deflector excitations correspond to compensated deflection distortion.

Conclusions

We have devised a method of decreasing the deflection aberrations significantly by minimizing the two most severe ones, field curvature and astigmatism, using one dynamic focus lens and one dynamic stigmator. Methods published so far eliminate each order of these aberrations separately using a dynamic lens and a stigmator per aberration order. The method presented here minimizes all orders of field curvature and astigmatism simultaneously without adding any correcting optical components, it only modifies the driving signal dependencies. For the example optical system with a shifted pivot point, the former approach would produce aberration sizes of $1.01 \mu\text{m}$ in a 1mm field of view (with the deflection distortion corrected), whereas our method almost halves that value to $0.535 \mu\text{m}$. In an ESEM, the method enables the use of smaller environmental distances and very small apertures without significantly limiting the field of view at low magnifications [13].

Aberration	Size / μm	
	Before	After
3rd order		
Spherical	0.00978	0.118
Coma	0.217	0.155
Field curvature	11.4	0.7
Astigmatism	5.06	1.29
Field curvature + astigmatism	16.5	1.99
All the above 3 rd order aberrations	16.5	1.91
5th order		
Spherical	0.000283	0.00528
Coma	0.0242	0.453
Field curvature	0.569	0.756
Astigmatism	0.355	2.01
Field curvature + astigmatism	0.924	2.77
Other 5 th order aberrations	0.0105	0.463
All 5 th order aberrations	0.924	2.77
3rd + 5th order		
Spherical	0.00966	0.114
Coma	0.24	0.137
Field Curvature	12.0	0.201
Astigmatism	5.41	0.0924
Field curvature + astigmatism	17.4	0.294
All 3 rd and 5 th order aberrations	17.3	0.535
All minus 3 rd order field curvature and astigmatism	1.01	

Table 1. Axial aberration sizes (minus deflection distortion, which has been compensated) before and after the minimization of all orders of field curvature and astigmatism in the upper-right corner of a 1mm field of view. The 7th order, which was also taken into account, is not listed due to space constraints and also because it is already less significant. The values in bold type: the value showing all aberrations minus the 3rd order field curvature and astigmatism represents the situation with these aberrations eliminated, whereas the other value shows the size of the overall aberration achieved by minimizing all orders of the two aberration types.

References:

- [1] PW Hawkes and E Kasper in “Principles of Electron Optics”, (Academic Press), (1994).
- [2] E Goto and T Soma, *Optik* **48** (1977), p. 255.
- [3] B Lencová, *Optik* **58** (1981), p. 25.
- [4] G D Danilatos, US patent No. 6809322 B2 (2004), also known as US 20030168595 A1.
- [5] GD Danilatos, J Rattenberger and V Dracopoulos, *J. Microsc.* **242** (2011), p. 166.
- [6] X Zhu, H Liu and E Munro, *Proc. SPIE* **2522** (1995), p. 66.
- [7] X Zhu *et al*, *Proc. SPIE* **3155** (1997), p. 47.
- [8] E Munro, *Optik* **39** (1974), p. 450.
- [9] LP Wang *et al*, *Optik* **113** (2002), p. 181.
- [10] H Kangyan and TT Tang, *Optik* **110** (1999), p. 9.
- [11] M Oral and B Lencová, *Ultramicroscopy* **109** (2009), p. 1365.
- [12] B Lencová and J Zlámál, *Phys. Procedia* **1** (2008), p. 315.
- [13] Supported by the Grant Agency of the Czech Republic, Project No. GA14-22777S and by Ministry of Education, Youth and Sports of the Czech Republic (LO1212).